Super-resolution reconstruction from truncated Hankel transform

Fedor Goncharov, Mikhail Isaev, Roman Novikov, Rodion Zaytsev

Super-resolution reconstruction from truncated Hankel transform

Fedor Goncharov, Mikhail Isaev, Roman Novikov, Rodion Zaytsev

Abstract We present the algorithm from our recent work Goncharov, Isaev, Novikov, Zaytsev (ArXiv preprint, 2024) for recovering a compactly supported function on $\mathbb{R}_+$ from its Hankel transform given on a finite interval $[0,r]$. This work employs the PSWF-Radon approach that combines the theory of classical one-dimensional prolate spheroidal wave functions with the Radon transform theory, which was originally developed for reconstructing signals from their truncated Fourier transforms. Adapted to the Hankel transform, it achieves what is known as 'super-resolution' (the ability to recover details smaller than π/r), even in the presence of moderate noise in the data. In particular, our numerical examples show that the PSWF-Radon approach is consistently as good as, and often outperforms, the conventional approach that complements missing data with zeros. In this review, to illustrate the efficiency of our algorithm to simultaneously operate with the Hankel transform of several different orders, we also include a new application involving truncated multiple angle expansions for functions on $\mathbb{R}^2$.

Fedor Goncharov
Université Paris Saclay, CEA, LIST, F-91120, Palaiseau-France
e-mail: fedor.goncharov@cea.fr

Mikhail Isaev
School of Mathematics and Statistics, UNSW Sydney, Sydney, NSW, Australia
e-mail: isaev.m.i@gmail.com

Roman Novikov
CMAP, CNRS Ecole polytechnique, Institut de Polytechnique de Paris, Palaiseau, France
e-mail: novikov@cmap.polytechnique.fr

Rodion Zaytsev
Faculty of Mathematics, HSE University, Igor Krichever Center for Advanced Studies
Skolkovo Institute of Science and Technology, Moscow, Russia
e-mail: rvzaytsev@edu.hse.ru

Key words: Hankel transform; Fourier transform; Radon transform; prolate spheroidal wave functions; super-resolution.
MSC2020: 42A38; 49K40; 33E10.

1.1 Introduction

The Hankel transform of order ν is defined by

$$H_\nu f(t) = \int_0^\infty f(s) J_\nu(ts)\sqrt{ts}\,ds,\ t \in \mathbb{R}_+, \tag{1.1}$$

where J_ν is the Bessel function of the first kind and $R_+ = [0,+\infty)$, $\nu \geq -\frac{1}{2}$. In particular, these assumptions imply that H_ν is invertible on $L^2(\mathbb{R}_+)$ and $H_\nu^{-1} = H_\nu$.

We consider the following problem.

Problem 1 Let $\sigma, r > 0$ and $\nu \geq -\frac{1}{2}$ be fixed. Find $f \in L^2(\mathbb{R}_+)$ from $h = H_\nu f$ given on $[0,r]$ (possibly with some noise), under a prior assumption that $\operatorname{supp} f \subset [0,\sigma]$.

Since $h(t)$ is real-analytic on $(0,\infty)$, theoretically one can solve Problem 1 using analytic continuation of $h(t)$: after recovery of $h(t)$ for $t \in \mathbb{R}_+$, we get $f = H_\nu h$. At the same time, it is known that analytic continuation for this geometry is exponentially unstable for any fixed σ and r; see [3] and references therein. Importantly, analytic continuation is not easy to implement numerically and to regularise; for some examples of algorithms see [12].

Another approach to Problem 1 is an approximate solution $f \approx f_{naive}$, where

$$f_{naive} = H_\nu \tilde{h}, \quad \tilde{h}|_{[0,\sigma]} = h, \quad \tilde{h}|_{(\sigma,\infty)} = 0. \tag{1.2}$$

It is well-known that reconstructions based on (1.2) fail to distinguish details smaller than *the diffraction limit* (of order π/r or less) because data for high frequencies was extrapolated with zeros. Despite this, this approach is widespread in industrial applications due to its noise robustness. In literature, reconstructing details beyond the diffraction limit is known as *super-resolution*. Similarly to analytic continuation, it is commonly accompanied by severe instability (unless substantial a priori information is available); see for example [4, 5, 6] and references therein.

In our recent work [3], we implement and adapt the PSWF-Radon approach, originally introduced in [4, 5] for the problem of band-limited Fourier inversion, to tackle Problem 1. The proposed algorithm is simple to implement as it relies only on standard libraries, moreover, it achieves super-resolution even for moderate levels of noise in data (in absence of noise – reconstructions are, at least theoretically, exact) and, most importantly, requires no manual tuning of its hyperparameters.

As an illustration we include [3, Figure 1.1] above as Figure 1.1. We refer to [3] for additional experiments and theoretical analysis of the PSWF-Radon approach

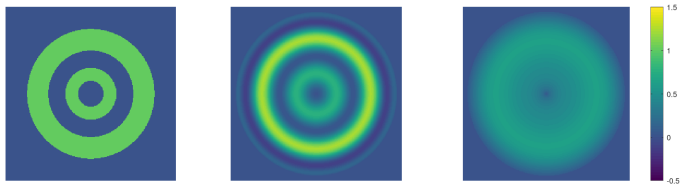

(a) (b) (c)

Fig. 1.1: An example from [3] for Problem 1 with $\nu = 0$, $\sigma = 1$, and $r = 10$: (a) preimage, (b) PSWF-Radon approach, (c) reconstruction via (1.2).

adapted to Problem 1. In particular, this work gives explicit Cormack-type reconstruction formulas, numerical experiments on stability, and examples of a stable super-resolution for orders $\nu \in \mathbb{N} = \{0, 1, 2, \ldots\}$ and $\nu \in \frac{1}{2} + \mathbb{N}$. Note also that our numerical experiments show that the PSWF-Radon approach is always superior to reconstructions based on (1.2), reaching similar quality for high levels of noise without any blow-ups.

This review focuses on the case of $\nu \in \mathbb{N}$ and highlights the simplicity of implementing algorithms based on the PSWF-Radon approach. Compared to [3], we include an additional numerical test that requires solving Problem 1 for several orders ν simultaneously: recovering a compactly supported function on $\mathbb{R}^2$ from the truncated multipole angle expansion of its Fourier transform.

We organise this review as follows. In Section 1.2, we introduce all necessary notations, explain the reduction of Problem 1 to band-limited Fourier inversion, and recall some basic facts of the theory of *prolate spheroidal wave functions* (PSWFs). In Section 1.3, we give the reconstruction algorithm from [3] for solving Problem 1 based on the PSWF-Radon approach. Finally, in Section 1.4, we present and discuss the aforementioned numerical experiment.

1.2 Preliminaries

For f in Problem 1 the following formula holds (see [3, Section 2.1]):

$$Fu(p) = \frac{1}{(2\pi)^2} \int_{\mathbb{R}^2} u(q) e^{i(q,p)}\, dq = \frac{i^\nu e^{i\nu\varphi_p}}{2\pi\sqrt{|p|}} H_\nu f(|p|),\ |p| \le r, \tag{1.3}$$

where

$$u(q) := \frac{f(|q|)}{\sqrt{|q|}} e^{i\nu\varphi_q},\ \frac{q}{|q|} = (\cos\varphi_q, \sin\varphi_q),\ q \in \mathbb{R}^2. \tag{1.4}$$

Using (1.3), (1.4), we reduce Problem 1 for $\nu \in \mathbb{N}$ to the following more general problem.

Problem 2 Let $r, \sigma > 0$ be fixed. Find $u \in L^2(\mathbb{R}^2)$ from Fu given on B_r (possibly with some noise), under a prior assumption that $\operatorname{supp} u \subset B_\sigma$.

Problem 2 is at the origin of the the PSWF-Radon approach in [4]. To model data in Problem 2 one uses, in particular, the truncated Fourier transform

$$F_c f(x) := \int_{-1}^{1} e^{icxy} f(y)\, dy, x \in [-1,1], c > 0, \tag{1.5}$$

where c is the "cut-off frequency". Operator F_c in (1.5) is well-known in theory of signal processing; see for example [1], [8], [11], [13], and references therein.

It is easy to verify that $F_c : L^2[-1,1] \to L^2[-1,1]$ is compact and not self-adjoint. One notable fact is that F_c has the following singular value decomposition:

$$F_c f(x) = \sum_{n\in\mathbb{N}} \mu_{n,c} \psi_{n,c}(x) \int_{-1}^{1} \psi_{n,c}(y) f(y)\, dy,$$

where $\{\psi_{n,c}\}_{n\in\mathbb{N}}$ are known as *prolate spheroidal wave functions*, $\{\mu_{n,c}\}_{n\in\mathbb{N}}$ are the corresponding eigenvalues; see [10], [7] and references therein. Collection $\{\psi_{j,c}\}_{j\in\mathbb{N}}$ constitutes an orthonormal basis in $L^2[-1,1]$, hence, the inverse F_c^{-1} (on range of F_c) is given by the formula:

$$F_c^{-1} g(y) = \sum_{n\in\mathbb{N}} \frac{1}{\mu_{n,c}} \psi_{n,c} \int_{-1}^{1} \psi_{n,c}(x) g(x)\, dx. \tag{1.6}$$

From compactness of F_c it follows that $\mu_{n,c} \to 0$ when $n \to \infty$. In practice this leads to numerical instability of computing $F_c^{-1} g$ when g is corrupted with noise and "falls off" the range of F_c. To approximate F_c^{-1} (in the weak sense) finite-rank operators $F_{n,c}^{-1}$ are used:

$$F_{n,c}^{-1} g(y) = \sum_{j=0}^{n} \frac{1}{\mu_{n,c}} \psi_{n,c} \int_{-1}^{1} \psi_{n,c}(x) g(x)\, dx, \tag{1.7}$$

where rank n is a free parameter used for regularisation. Note that for each $n \in \mathbb{N}$, operator $F_{n,c}^{-1}$ is well defined on $L^2[-1,1]$.

The principal source of instability in the PSWF-Radon approach of [3] is conditioning of $F_{n,c}^{-1}$ which is completely characterized by behavior of $\{\mu_{n,c}\}_{j\in\mathbb{N}}$. For example, it is known that (see [10, Section 3.2.3])

$0 < |\mu_{n+1,c}| < |\mu_{n,c}|$ for all $j \in \mathbb{N}$,
$\mu_{n,c}$ decay to zero with exponential rate when $j \to +\infty$.

Moreover, for fixed c there is "critical" $n_{crit,c} = \lfloor \frac{2c}{\pi} \rfloor$ so that $|\mu_{n,c}| \approx (2\pi/c)^{1/2}$ for $n < n_{c,crit}$ and there are approximately $\pi^{-2}\log((\frac{1}{\varepsilon_1}-1)/(\frac{1}{\varepsilon_2}-1))\log(c)$ eigenvalues with absolute values in interval $\sqrt{2\pi/c}\cdot[\varepsilon_1,\varepsilon_2]$, $\varepsilon_1,\varepsilon_2 \in (0,1)$. Therefore, on span of $\{\psi_{n,c} : n < n_{crit,c}\}$ inversion of F_c via $F^{-1}_{n_{crit},c}$ is very stable and there is an additional subspace of dimension $O(\log(c))$ where the corresponding stability may still be acceptable given the noise level in the input.

1.3 Reconstruction for Problem 1 from [3]

Recall from the previous section that Problem 1 is reduced to Problem 2 for u in (1.4) with truncated data given by (1.3). The PSWF-Radon approach for Problem 2 is based on the following identity [4, Theorem 1.4]:

$$\begin{aligned} &Fu(rx\theta) = \left(\frac{\sigma}{2\pi}\right)^2 F_c R_\theta u_\sigma(x),\ u_\sigma(q) = u(\sigma q),\ \operatorname{supp} u \subset B_1, \\ &x \in [-1,1],\ \theta \in \mathbb{S}^1,\ c = r\sigma, \end{aligned} \tag{1.8}$$

where R_θ is the classical Radon transform defined by the formula

$$R_\theta u(s) = \int\limits_{q\theta = s} u(q)\, dq.$$

Applying $F^{-1}_{n,c}$ (for appropriate n) and R^{-1} (Radon inverse) to both sides of (1.8) one recovers $u_n \approx u$. Finally, using (1.4) we obtain

$$f \approx f_n(s) = \frac{\sqrt{s}}{2\pi}\int\limits_0^{2\pi} u_n(s\cos\varphi, s\sin\varphi)e^{-i\nu\varphi}\, d\varphi,\ s \in [0,\sigma]. \tag{1.9}$$

Thus, for $\nu \in \mathbb{N}$ the reconstruction scheme for Problem 1 is as follows:

$$h \xrightarrow{(1.3)} Fu \xrightarrow{(1.8),\,(1.3)} F_c R_\theta u_\sigma \xrightarrow{(1.6),\,(1.7)\text{ and } R^{-1}} u_\sigma \xrightarrow{(1.9)} f. \tag{1.10}$$

For R^{-1} we use the classical FBP algorithm (see for example [9]), instead of F_c^{-1} we use $F^{-1}_{n,c}$ from (1.7). Regularisation parameter n is chosen automatically according to *residual minimisation principle*:

$$n = \operatorname{argmin}_{m\in\{0,\dots N_{\max}\}} \|H_\nu f_m - h\|_{L^2[0,r]}. \tag{1.11}$$

where f_m is a reconstruction by PSWF-Radon approach in (1.9).

Note that reconstructing f by (1.10) has the following attractive features:

+ only one-dimensional prolate spheroidal wave functions are required (many efficient libraries implement PSWFs in dimension one; see for example, [1], [2]);
+ all numerical operations are standard and implemented in corresponding libraries (e.g., Radon inversion in 2D, PSWFs in 1D) or require very little work in contrast to classical algorithms for analytic continuation;
+ for $n \to \infty$ reconstruction is exact, achieving super-resolution when $n > n_{crit,c}$, in contrast with f_{naive} from (1.2); see discussion in Section 1.2.

However, there is one potential bottleneck of our approach to improved:

- for dense grids single call of R^{-1} may require significant amount of computational resources: Problem 1 is one dimensional, whereas Problem 2, which we solve in (1.10), is two-dimensional (and three-dimensional for $\nu \in \frac{1}{2} + \mathbb{N}$; see [3]); note also that memory and time complexity grow exponentially with dimension.

1.4 Numerical experiment with multipole angle expansions

Given $u = u(q) \in L^2(\mathbb{R}^2)$, $\operatorname{supp} u \subset B_\sigma$, its multipole angle expansion and the Fourier transform Fu are given by (see [3, Section 2.1])

$$\begin{aligned} u(q) &= \sum_{k\in\mathbb{Z}} u_k(|q|)e^{ik\varphi_q},\ \frac{q}{|q|} = (\cos\varphi_q, \sin\varphi_q),\ \varphi_q \in [0, 2\pi), \\ Fu(p) &= \frac{1}{2\pi\sqrt{|p|}} \sum_{k\in\mathbb{Z}} i^k H_k f_k(|p|)e^{ik\varphi_p},\ p \in \mathbb{R}^2 \backslash \{0\}, \end{aligned} \tag{1.12}$$

where

$$f_k(s) := u_k(s) \cdot \sqrt{s},\ s \in \mathbb{R}_+. \tag{1.13}$$

After truncation we consider that

$$H_\nu f_\nu(t),\ t \in [0, r],\ \nu \in \{0, \dots, K\} \text{ are known.}$$

We solve Problem 1 for each $\nu \in \{0, \dots, K\}$ by recovering f_k for $k \in \{-K, \dots, K\}$ (note that $H_{-\nu} f = (-1)^\nu H_\nu f$) and consequently u_k using (1.13). Then, the final recovery is obtained in form of truncated multipole angle expansion in (1.12) using previously recovered u_k.

Results of our numerical experiment are presented in Figures 1.2, 1.3. We set $\sigma = 1$, $r = 15$. Three disks in the phantom u have diameters $\{0.26, 0.26, 0.28\}$ with $u = 1$ inside the disk and $u = 0$ otherwise. Distances between boundaries of disks are $\{0.08, 0.08, 0.06\}$; see Figure 1.2 (a). In Figure 1.2 (b) we also present the truncated multipole angle expansion of order $K = 20$ which approximates the phantom. Using only $H_k f_k$, $|k| \le K$, an algorithm can recover, at best, this approximation but not the original phantom. Note that diameters of disks are slightly larger than the diffraction

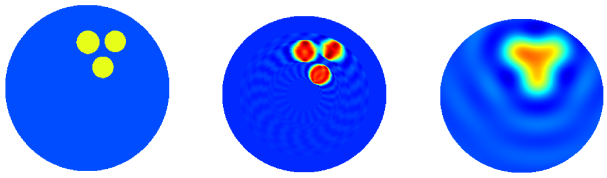

(a) (b) (c)

Fig. 1.2: (a) three-disks phantom; (b) its truncated angle multipole approximation of order $K = 20$; (c) reconstruction via (1.2)

limit $\pi/r \approx 0.21$, whereas distances between them are essentially smaller. Therefore, without super-resolution it is impossible to resolve three disks and, indeed, the conventional reconstruction by (1.2) fails to do so; see Figure 1.2 (c).

The PSWF-Radon algorithm achieves super-resolution for the example from Figure 1.2 with additive Gaussian white noise up to 30%; see Figure 1.3. We also highlight that it is fully automatized: given $H_\nu f = h$ from Problem 1, the only free parameter n in $F_{n,c}^{-1}$ is chosen by the residual minimisation principle in (1.11) with $N_{\max} = 30$. For equispaced grids of 256 points on $[0,r]$, $[0,\sigma]$, a single reconstruction of u_k on a laptop with CPU AMD 7 7840, using 16 threads, took approximately 10 seconds, thus taking ~ 200 seconds to recover u (memory usage was negligible). For a detailed analysis of numerical complexity of the PSWF-Radon algorithm we refer to [**?**, Section 3].

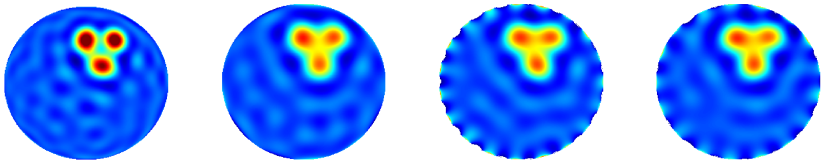

(a) (b) (c) (d)

Fig. 1.3: PSWF-Radon reconstructions with n chosen according to (1.11) for the following noise levels: (a) 0%, (b) 10%, (c) 20%, (d) 30%.

Interestingly, using residual minimisation rule (1.11), we never observed overfitting to noise in reconstructions (which is generally common for ill-posed inverse problems). At worst, for high levels of noise the conventional approach via (1.2) and the PSWF-Radon approach become comparable which is definitely a positive feature of the latter. Additional numerical experiments (not shown here) also demonstrated that achieved super-resolution is sensitive to size of detail we want to resolve.

For example, if distances between disks are decreased by 20%, then super-resolution is achievable only for noise levels below 5%; see [3, Section 3] for more detail.

Overall, our experiment demonstrates that PSWF-Radon approach has enough stability for $\nu \in \{0, 1, \ldots, 20\}$ to be superior or, at least, comparable to the conventional approach based on (1.2). The code is based on implementation from [3, Section 3], which is open-access available at *https://github.com/fedor-goncharov/pswf-radon*.

References

1. Adelman, R., Gumerov, N., Duraiswami, R.: Sowftare for computing spheroidal wave functions using arbitrary precision arithmetic. arXiv:1408.0074 (2014)
2. Driscoll, T., Hale, N., Trefethen, L.: Chebfun guide (2014)
3. Goncharov, F., Isaev, M., Novikov, R., Zaytsev, R.: PSWF-Radon approach to reconstruction from band-limited Hankel transform. arXiv:2409.17409 (2024)
4. Isaev, M., Novikov, R.: Reconstruction from the Fourier transform on the ball via prolate spheroidal wave functions. Journal de Mathématiques Pures et Appliquées **163**, 318–333 (2022)
5. Isaev, M., Novikov, R., Sabinin, G.: Numerical reconstruction from the Fourier transform on the ball using prolate spheroidal wave functions. Inverse Problems **38**(10):105002 (2022).
6. Isaev, M., Novikov, R., Sabinin, G.: Super-resolution reconstruction from truncated Fourier transform. Extended Abstracts MWCAPDE 2023: Methusalem Workshop on Classical Analysis and Partial Differential Equations, p.63 Springer Nature (2024)
7. Karoui, A.: Uncertainty Principles, Prolate Spheroidal Wave Functions and Applications. Recent Developements in Fractals and Related Fields, 165–190 (2010)
8. Landau, H., Pollak, H.: Prolate spheroidal wave functions, Fourier analysis and uncertainty – III: the dimension of the space of essentially time-and band-limited signals. Bell System Technical Journal **41**(4), 1295–1336 (1962)
9. Natterer, F.: The Mathematics of Computerized Tomography., SIAM (2001)
10. Osipov, A., Rokhlin, V., Xiao, H.: Prolate Spheroidal Wave Functions of Order Zero: Mathematical Tools for Bandlimited Approximations. Springer Ser. Appl. Math. Sci 187 (2013)
11. Slepian, D., Pollak, O.: Prolate spheroidal wave functions, Fourier analysis and uncertainty – I. Bell System Technical Journal **40**(1), 43–63 (1961)
12. Trefethen, L.: Numerical analaytic continuation. Japan Journal of Industrial and Applied Mathematics **40**(3), 1587–1636 (2023)
13. Levitina, T., Brändas, E.: Computational techniques for prolate spheroidal wave functions in signal processing **1**(2-3), 287–313 (2001)